JP2.3

The diurnal cycle of radiative fluxes using 3D stratocumulus cloud fields from Large-Eddy simulations

S.R. de Roode* **and A. Los**
Royal Netherlands Meteorological Institute, The Netherlands

1. Introduction

The albedo of a plane parallel cloud is larger than for a horizontally inhomogeneous cloud having the same mean optical depth (Cahalan et al. 1994). In the ECMWF weather forecast model this so-called plane parallel homogeneous (PPH) albedo bias effect is taken into acount by decreasing the mean liquid water path (LWP) by a cloud inhomogeneity correction factor $\chi = 0.7$. This gives an *effective* liquid water path LWP_{eff} which is used in the solar radiation scheme,

$$LWP_{eff} = \chi LWP. \tag{1}$$

The value of the albedo bias depends substantially on the horizontal variability of the cloud optical depth τ, which may be measured by its variance $\overline{\tau'^2}$ (Los and Duynkerke 2001). An LES study of the diurnal cycle of stratocumulus (Duynkerke et al. 2004) shows that the total humidity field in the middle of the cloud layer correlates very well with the cloud liquid water path (see Figure 1). This motivates the following question:

Is it possible to link the variance of the total water specific humidity to the cloud inhomogeneity correction factor χ?

* *Corresponding author address:* Stephan de Roode, KNMI, KS/AO, P.O. box 201, 3730 AE De Bilt, The Netherlands, roode@knmi.nl

In general, the microphysical and macrophysical properties of the cloud will determine the cloud optical depth. Because the ECMWF model uses a constant value for the cloud droplet effective radius r_e in warm stratocumulus clouds, the LWP and the cloud optical depth are linearly related (Stephens 1984),

$$\tau = \frac{3}{2}\frac{LWP}{\rho_l r_e}, \tag{2}$$

with ρ_l the density of liquid water. Figure 2 shows a schematic illustration of the dependency of the cloud inhomogeneity factor χ on the variance of the total specific humidity and temperature. An algorithm to compute the variance of the total specific humidity in a cloud layer is presented by Tompkins (2001) and has been incorporated in the ECMWF model physics package. Note that Los and Duynkerke (2000) discuss a more general relation between fluctuations in the liquid water content and the cloud optical depth in case cloud droplet sizes are allowed to vary with height.

Recent studies of satellite observations (Pincus et al. 1999) and Large-Eddy simulations (Bäuml et al. 2004) report a smaller albedo bias than Cahalan et al. (1994). The Large-Eddy Simulations (LES) study also shows that the albedo bias varies for two different stratocumulus cases. We will analyse LES results of the diurnal cycle of FIRE I stratocumulus to show

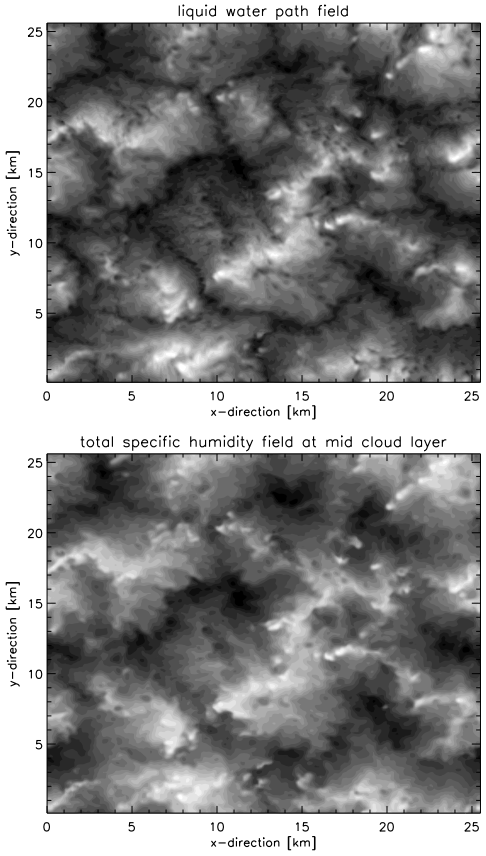

Figure 1: Grey-scale plot of the instantaneous liquid water path and total water specific humidity fields in the middle of a stratocumulus cloud layer after 10 hours of simulation time on a large horizontal domain (25.6 $\times$ 25.6 km^2). The fields were obtained from a Large-Eddy Simulation of the diurnal cycle of stratocumulus off the coast of California as observed during FIRE I as part of the EUROCS project. The results indicate that the large-scale structures are nearly identical.

that the cloud inhomogeneity correction factor χ exhibits temporal variations. In addition, following the schematic (Fig. 2) we will derive an analytic expression that gives LWP fluctuations as a function of total humidity fluctuations.

2. The diurnal cycle of the stratocumulus albedo bias from a Large-Eddy Simulation

To investigate if there is any diurnal cycle in the albedo bias we have re-run the FIRE I stratocumulus case with the dutch LES model using a reduced 6.4×6.4 km^2 horizontal domain with 100 (20) m horizontal (vertical) grid resolution. The initial (thermo-) dynamic state was determined from radiosonde observations of temperature and relative humidity vertical profiles collected during the FIRE I stratocumulus experiment (Duynkerke et al. 2004). The simulated diurnal cycle of the stratocumulus liquid water path is shown in Figure 4. As a result of solar radiative absorption the cloud deck tends to thin during the day and thickens during the night.

The probability density function (PDF) of the LWP during nighttime and day-time is presented in Figure 3. During nighttime the convection is driven by longwave radiative cooling near the top of the cloud. The PDF of the liquid water path shows an elongated tail towards small values. These liquid water reductions are due to entrainment of relative warm and dry air parcels from above the inversion. In contrast, during daytime shallow cumuli transport relatively moist air from the surface to a relatively thin stratocumulus layer above explaining the tail in the PDF toward relatively large LWP values.

Two radiative transfer models were applied to compute albedos, the delta-Eddington radiative transfer equation, and the I3RC Monte Carlo model. To focus the comparisons on the cloud inhomogeneity effects we used a fixed solar zenith angle $\theta_0 = 53°$, a fixed cloud droplet effective radius $r_e = 10\mu$, and a single scattering albedo allowing radiative absorption in the cloud (Fouquart 1985). More details on the boundary conditions and the model parameters can be found in Duynkerke et al. (2004) for the delta-Eddington method and in Cahalan et al. (2005) for the I3RC Monte Carlo model.

Based on hourly instantaneous LWP fields of stratocumulus we computed the albedo (A_{PPH}) for a plane-parallel cloud having a mean optical thick-

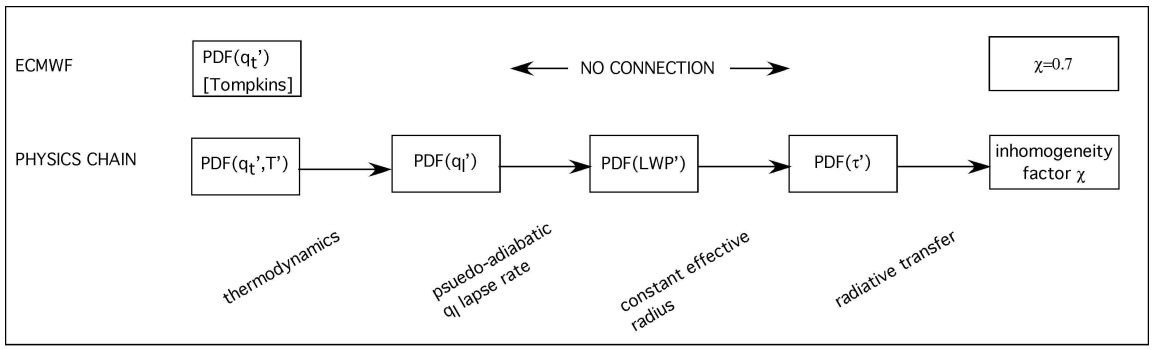

Figure 2: Schematic showing how in-cloud fluctuations of the temperature T and total specific humidity q_t determine the cloud inhomogeneity correction factor χ assuming a constant effective radius. The quantity q_l denotes the liquid water content, and a prime symbol indicates fluctuations with respect to the horizontal slab-mean value. Currently, the ECMWF model computes the PDF of the total specific humidity according to Tompkins (2001).

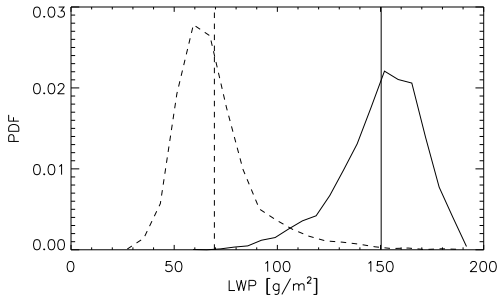

Figure 3: PDFs of the liquid water path at 4 h Local Time (nighttime, solid line) and 16 h Local Time (day-time, dashed line). The vertical lines indicate the mean values.

ness $\overline{\tau}$. With the delta-Eddington radiative transfer equation we calculated the albedo for every single cloud column (the "independent column approximation (ICA)") for all LWP fields. From the I3RC Monte Carlo model we obtained the albedo using the full 3 dimensional structure of all liquid water content fields, while all other parameters were the same as in the delta-Eddington calculations. We then slab-averaged the albedo of each column to obtain the mean albedo for a horizontally inhomogeneous cloud (A_{ICA} and A_{I3RC}, respectively).

The cloud inhomogeneity correction factor χ was determined by finding the optical depth τ_{eff} for which its plane parallel albedo corresponds to the mean albedo for a horizontally inhomogeneous cloud, $A(\tau_{eff}) = A_{ICA}$ or $A(\tau_{eff}) = A_{I3RC}$ such that

$$\chi = \frac{\tau_{eff}}{\overline{\tau}}. \tag{3}$$

Note that only for a constant r_e the definition of χ given in Eq. (1) is identical to the one defined by Eq. (3).

According to Figure 5 the factor χ has a minimum value ~ 0.93 during daytime when the cloud depth is minimum, independently of the radiative transfer model (solid line: ICA, dashed line I3RC). For χ values close to unity the I3RC results are scattered around the results obtained from the ICA calculations. This could be due to mean absorptivity changes in 3 dimentional inhomogeneous cloud fields.

Because we used a fixed solar zenith angle to compute the cloud albedo, the temporal variations in χ are due to variations in the mean and the variance of the LWP. For an optically thick cloud the cloud inhomogeneity correction factor χ is near unity indicating that the albedo bias is insignificant. For an optically thin cloud the albedo bias becomes more important, although the LES results suggest that the value for χ should be much larger than the value of 0.7 currently used in the ECMWF model.

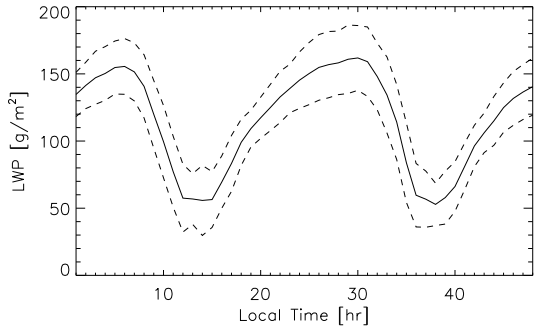

Figure 4: The diurnal cycle of the mean liquid water path (thick line) from a Large-Eddy Simulation of stratocumulus. The dashed lines represent one standard deviation ($\sigma_{LWP} = \sqrt{\overline{LWP'^2}}$) from the mean. The cloud-top height was located around 600 m, and variations in the cloud depth could be predominantly attributed to variations in the cloud-base height.

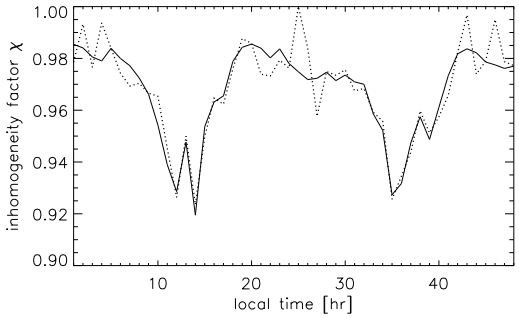

Figure 5: The cloud inhomogeneity correction factor χ computed from the diurnal cycle of stratocumulus clouds. Solid line: computed using the delta-Eddington radiative transfer equation. Dotted line: obtained with the I3RC Monte Carlo model. A fixed solar zenith angle $\theta_0 = 53^\circ$ was used.

3. Construction of the PDF for the liquid water path

Here we derive an analytic expression to relate q_t to LWP fluctuations. Liquid water content fluctuations q_l' are given by

$$q_l' = q_t' - q_{sat}'. \tag{4}$$

Hence to obtain q_l' fluctuations given q_t' fluctuations, one needs to know the fluctuations of the saturated specific humidity q_{sat}'. For a saturated atmosphere we can use Clausius-Clapeyron (Nicholls 1984)

$$q_{sat}' = \left(\frac{dq_{sat}}{dT}\right) T'. \tag{5}$$

If we make a scatter plot of T' and q_t' fluctuations from the LES results, it appears that all points fall approximately along a straight line. Therefore, temperature fluctuations may be expressed as $T' = c_{qT} q_t'$. If we estimate the slope factor c_{qT} from the conditionally sampled mean updraft $(q_{t,u}, T_u)$ and downdraft values $(q_{t,d}, T_d)$,

$$c_{qT} = \frac{T_u - T_d}{q_{t,u} - q_{t,d}}, \tag{6}$$

and if we use that the conditionally sampled flux for an arbitrary quantity ψ is well correlated to the total turbulent flux,

$$\overline{w'\psi'} \approx \frac{1}{c} M_c (\psi_u - \psi_d), \tag{7}$$

where M_c the updraft mass flux and c a proportionality factor which is observed to have a typical value ~ 0.6 in stratocumulus and clear convective boundary layers (de Laat and Duynkerke 1998), then the slope factor can be computed directly from vertical fluxes,

$$c_{qT} = \frac{T_u - T_d}{q_{t,u} - q_{t,d}} = \frac{M_c (T_u - T_d)}{M_c (q_{t,u} - q_{t,d})} \approx \frac{\overline{w'T'}}{\overline{w'q_t'}}. \tag{8}$$

Note that the temperature and humidity fluxes are routinely computed in GCMs. With aid of Eqs. (5) and (8) liquid water content fluctuations can be expressed as

$$q_l' = q_t' \left[1 - \left(\frac{dq_{sat}}{dT}\right) c_{qT}\right] \equiv \beta q_t'. \tag{9}$$

The factor β depends weakly on the mean temperature, and on the ratio of the temperature to total humidity fluctuations. For the simulation of the stratocumulus diurnal cycle we find $\beta \approx 0.5$.

In a model the vertical distribution of liquid water content fluctuations in a cloud column is not known. To circumvent this problem, we will assume that the mean vertical gradient of the liquid water content (α) applies to every single cloud column (see for a

schematic illustration Figure 6). A similar assumption was made by Los and Duynkerke (2000) who used the wet-adiabatic liquid water lapse rate to describe the vertical structure of the cloud field. Instead, we will use a "pseudo-adiabatic" liquid water lapse rate that is based on the actual modeled liquid water content vertical profile. The linear vertical liquid water content profile reads

$$q_l(z) = \alpha(z - z_b), \tag{10}$$

with z_b the cloud-base height. The cloud liquid water path is defined by

$$\overline{LWP} = \rho_0 \int_{z_b}^{z_t} \overline{q_l}(z)dz, \tag{11}$$

with ρ_0 the mean air density (which is necessary if q_l has units kg/kg), and z_t the cloud-top height. For a linear liquid water content profile we can write

$$\overline{LWP} = \frac{\rho_0 \alpha \overline{H}^2}{2} \quad \Longleftrightarrow \quad \alpha = \frac{2\overline{LWP}}{\rho_0 \overline{H}^2}, \tag{12}$$

with the mean cloud-layer depth $\overline{H} = z_t - z_b$. Using Eqs. (10) and (12) we define the mean maximum liquid water content,

$$\overline{q_l}_{max} = \alpha \overline{H} = \sqrt{\frac{2\alpha \overline{LWP}}{\rho_0}}. \tag{13}$$

The constant liquid water content lapse rate α implies that q_l' fluctuations in a cloud column must be constant with height. Observations near the top of stratocumulus clouds show that cloud-top height variations are relatively small. Like Los and Duynkerke (2000) we assume that all cloud-columns have the same cloud-top height. This allows to write the local maximum liquid water content as

$$q_{lmax} = \overline{q_l}_{max} + q_l'. \tag{14}$$

Using Eqs. (10) and (14) the local cloud-layer depth $H = \overline{H} + H'$ can be expressed as

$$H = \frac{\overline{q_l}_{max} + q_l'}{\alpha}. \tag{15}$$

Note that the fluctuation in the cloud depth H' is proportional to q_t',

$$\frac{H'}{\overline{H}} = \frac{q_t'}{\overline{q_l}_{max}}, \tag{16}$$

Like Eq. (12), we can express the local cloud liquid water path $LWP = \overline{LWP} + LWP'$,

$$LWP = \frac{\rho_0 \alpha H^2}{2}. \tag{17}$$

With aid of Eqs.(9), (12), (13) and (15) we rewrite Eq. (17) to give an expression for the fluctuating part of the LWP,

$$LWP' = \rho_0 \overline{H} \beta q_t' + \frac{\rho_0 \overline{H} \beta^2 {q_t'}^2}{2\overline{q_l}_{max}}. \tag{18}$$

Or, as an alternative, if we use Eq. (16) we can write

$$LWP' = \rho_0 \overline{H} \beta q_t' + \frac{\rho_0 H' \beta^2 q_t'}{2}. \tag{19}$$

If $\beta > 1$, then cloud columns are relatively moist and cold (or dry and warm), causing liquid water path fluctuations to be enhanced by the temperature effect, and vice versa for $\beta < 1$. If the temperature fluctuations would be negligibly small, or if the saturation specific humidity would not depend on the temperature, then $\beta = 1$. In that case the first term on the rhs of Eq. (19) gives $LWP' = \rho_0 \overline{H} q_t'$. This is the solution for a vertically homogeneous cloud column having a depth $\overline{H}$ and liquid water content q_t'. Likewise the second term yields $LWP' = \rho_0 H' q_t'/2$, which explains fluctuations in the LWP due to a local fluctuation in the cloud layer depth H', having a linear liquid water vertical profile and a maximum liquid water content q_t' (see Figure 6).

Examples of actual and constructed PDFs for the LWP fluctuations are shown in Figure 7. We used the PDF for q_t computed from LES results at a height of 440 m which is approximately in the middle of the cloud layer. It is clear that the first term on the rhs of Eq. (18) compares satisfactorily well with the PDF of the LWP computed directly from the actual liquid water content field. This means that the cloud-base height fluctuations are relatively small. If we use $\beta = 1$ then we find a PDF for the LWP that is too broad, indicating that it is necessary to take into account temperature fluctuations.

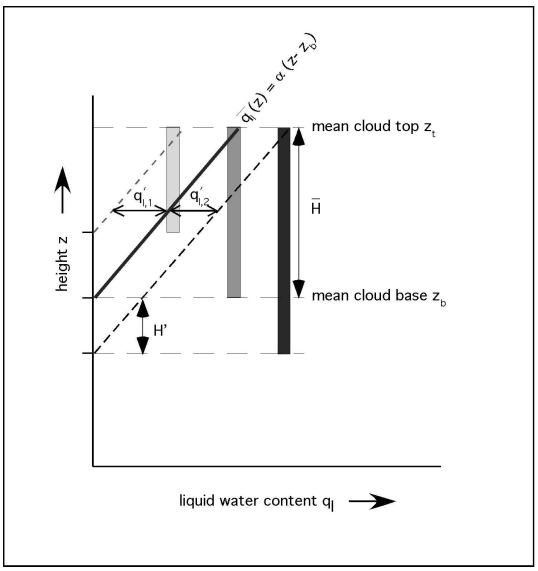

Figure 6: Schematic illustration of the mean state for which the mean liquid water content $\overline{q_l}$ follows a psuedo-adiabatic lapse rate with slope α. Given fluctuations of the liquid water content q_l' near the middle of the cloud layer, perturbed liquid water profiles are computed by assuming that they have the same slope α and an identical cloud-top height. A vertical integration of the perturbed liquid water vertical profiles yields the perturbed liquid water path.

4. Conclusions

LES results of the diurnal cycle of stratocumulus indicate that the cloud inhomogeneity correction factor depends critically on the mean and variance of the cloud liquid water path. For an optically thick cloud the albedo bias appears to be insignificant and seems most relevant to optically thin clouds ($\tau \lesssim 10$). Therefore, using a constant cloud inhomogeneity correction factor in a solar radiative transfer scheme seems rather crude. In a GCM the variations in the mean liquid water path can be directly computed from the liquid water field, but not its variance.

From a detailed analysis of LES fields of thermodynamic quantities, and application of some thermodynamic relations, a simple analytic formula is derived to give the PDF of the liquid water path as a function of the PDF of the total water specific humidity in the middle of the cloud layer. To arrive at this results we had to make two important assumptions, namely that cloud-top height variations are negligibly small, and that vertical liquid water profiles in subcolumns have identical mean vertical gradients. These assumptions may be fairly well applicable to a cloud deck having cloud fractions near unity, but their validity may possibly degrade for a very inhomogeneous cloud layer, for example a thin and broken stratocumulus layer penetrated by cumuli from below.

The cloud albedo bias is principly due to fluctuations in the cloud optical depth. If in a GCM the variance $\overline{q_t'^2}$ is computed, it can be straightforwardly converted to the variance of the LWP. If we neglect the second term on the rhs of Eq. (19), $\overline{LWP'^2}$ may be well approximated by

$$\overline{LWP'^2} = (\rho_0 \overline{H} \beta)^2 \overline{q_t'^2}. \tag{20}$$

For a constant cloud droplet effective radius the variance of the optical depth becomes,

$$\overline{\tau'^2} = \left(\frac{3\rho_0 \overline{H} \beta}{2\rho_l r_e} \right)^2 \overline{q_t'^2}, \tag{21}$$

where we used Eq. (2). To get a more accurate estimation of $\overline{\tau'^2}$, one needs to take into account the variation of microphysical properties with height. Suggestions to this end are given in Los and Duynkerke (2000).

References

Bäuml, G., A. Chlond, and E. Roeckner, 2004: Estimating the pph-bias for simulations of convective and stratiform clouds. *Atm. Res.*, **72**, 317–328.

Cahalan, R. F., L. Oreopoulos, A. Marshak, K. F. Evans, A. B. Davis, R. Pincus, K. H. Yetzer, B. Mayer, R. Davies, T. P. Ackerman, H. W. Barker, E. E.Clothiaux, R. E. Ellingson, M. J. Garay, E. Kassianov, S. Kinne, A. Macke, W. O'Hirok, P. T. Partain, S. M. Prigarin, A. N. Rublev, G. L. Stephens, F. Szczap, E. E. Takara, T. Vánai, G. Wen, , and T. B. Zhuravleva, 2005: The I3RC - bringing together the most advanced tools for radiative

transfer in cloudy atmospheres. *Bull. Am. Meteorol. Soc.*, 1275–1293.

Cahalan, R. F., W. Ridgway, W. J. Wiscombe, S. Gollmer, and Harshvardhan, 1994: Independent pixel and Monte-Carlo estimates of stratocumulus albedo. *J. Atmos. Sci.*, **51**, 3776–3790.

de Laat, A. T. J. and P. G. Duynkerke, 1998: Analysis of ASTEX-stratocumulus observational data using a mass-flux approach. *Boundary-Layer Meteorol.*, **86**, 63–87.

Duynkerke, P. G., S. R. de Roode, M. C. van Zanten, J. Calvo, J. Cuxart, S. Cheinet, A. Chlond, H. Grenier, P. J. Jonker, M. Köhler, G. Lenderink, D. Lewellen, C.-L. Lappen, A. P. Lock, C.-H. Moeng, F. Müller, D. Olmeda, J.-M. Piriou, E. Sanchez, and I. Sednev, 2004: Observations and numerical simulations of the diurnal cycle of the EUROCS stratocumulus case. *Q. J. R. Meteorol. Soc.*, **130**, 3269–3296.

Fouquart, Y.: 1985, Radiation in boundary layer clouds. *Report, JSC/CAS Workshop on Modelling of Cloud-Topped Boundary Layer*, Fort Collins, CO, WMO/TD 75, Appendix D, 40 pp.

Los, A. and P. G. Duynkerke, 2000: Microphysical and radiative properties of inhomogeneous stratocumulus: Observations and model simulations. *Q. J. R. Meteorol. Soc.*, **126**, 3287–3307.

— 2001: Parametrization of solar radiation in inhomogeneous stratocumulus: Albedo bias. *Q. J. R. Meteorol. Soc.*, **127**, 1593–1614.

Nicholls, S., 1984: The dynamics of stratocumulus: Aircraft observations and comparisons with a mixed layer model. *Q. J. R. Meteorol. Soc.*, **110**, 783–820.

Pincus, R., S. A. McFarlane, and S. A. Klein, 1999: Albedo bias and the horizontal variability of clouds in subtropical marine boundary layers: Observations from ship and satellites. *J. Geophys. Res.*, **104**, 6183–6191.

Stephens, G. L., 1984: The parameterization of radiation for numerical weather prediction and climate models. *Mon. Weather Rev.*, **112**, 826–867.

Tompkins, A. M., 2001: A prognostic parameterization for the subgrid-scale variability of water vapor and clouds in large-scale models and its use to diagnose cloud cover. *J. Atmos. Sci.*, **59**, 1917–1942.

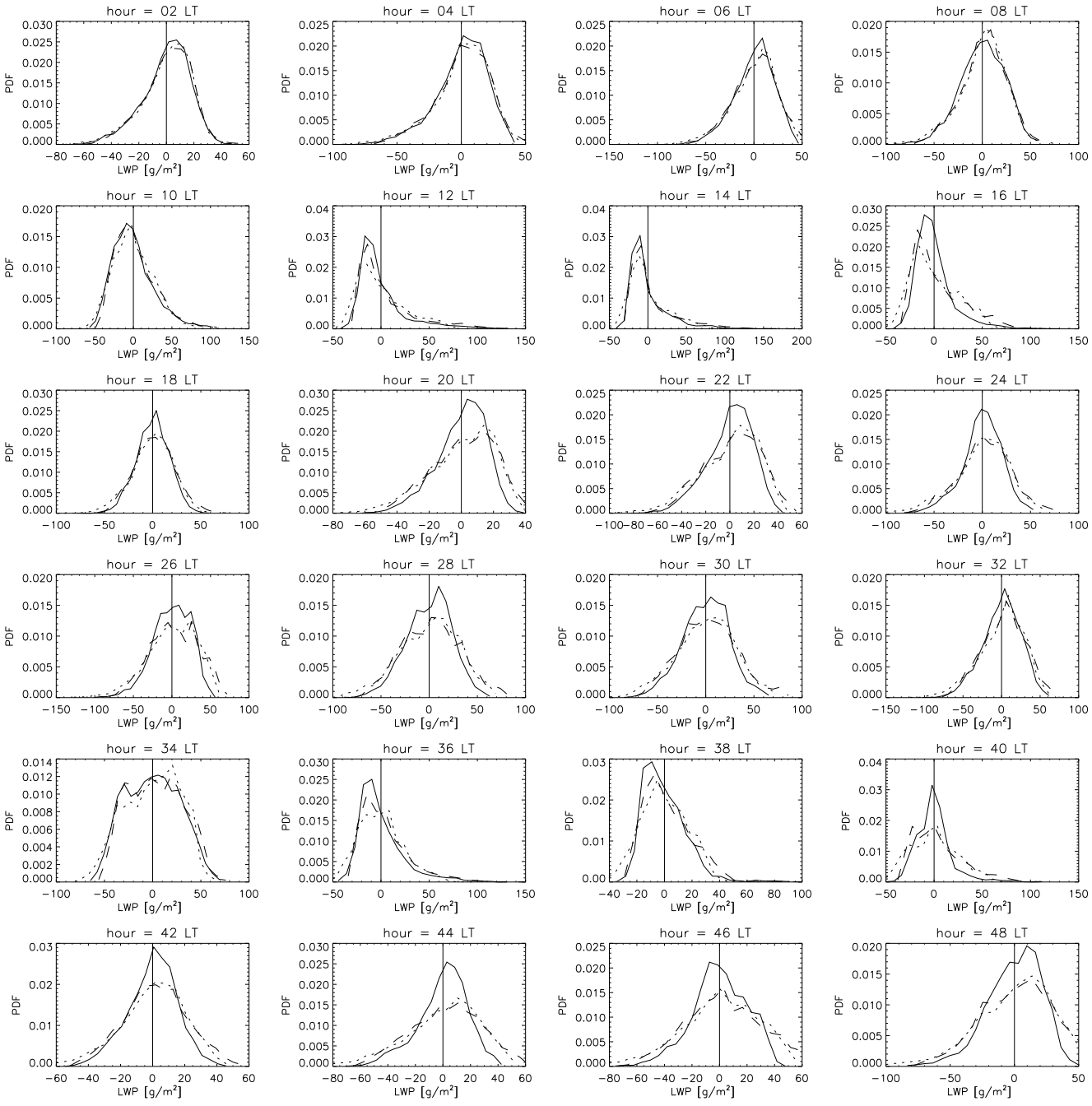

Figure 7: Thumbnail time series of the PDF(LWP') directly computed from the LES liquid water fields (solid line), and the constructed PDF from the full analytical solution Eq. 18 (dashed line), and the dotted line the solution using only the first term on the rhs of Eq. (18).